

**Cell Reports Methods, Volume 2**

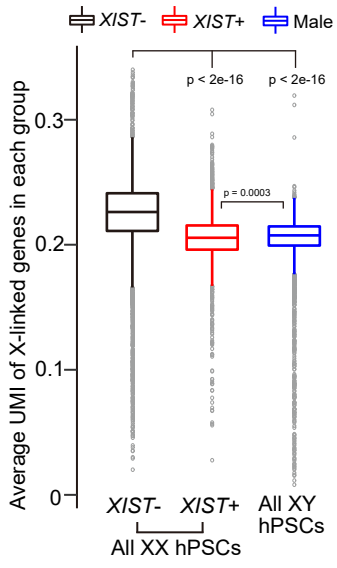
**Supplemental information**

**De-erosion of X chromosome dosage compensation  
by the editing of *XIST* regulatory regions  
restores the differentiation potential in hPSCs**

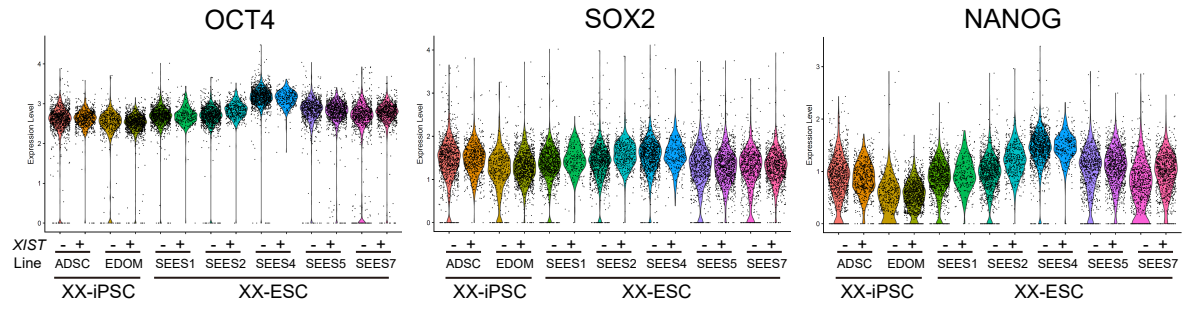
**Nami Motosugi, Akiko Sugiyama, Chisa Okada, Asako Otomo, Akihiro Umezawa, Hidenori Akutsu, Shinji Hadano, and Atsushi Fukuda**

**Figure S1**

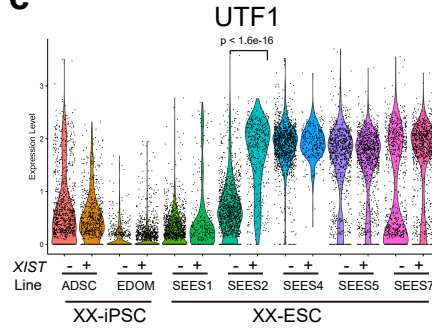
**a**



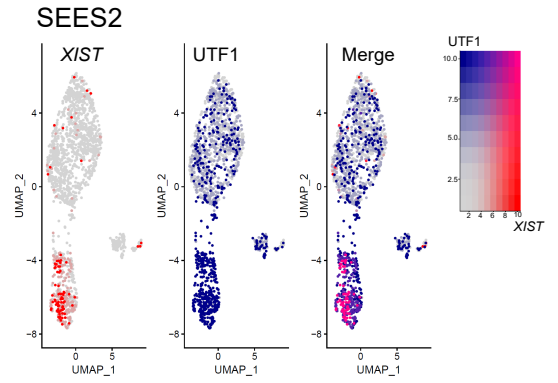
**b**



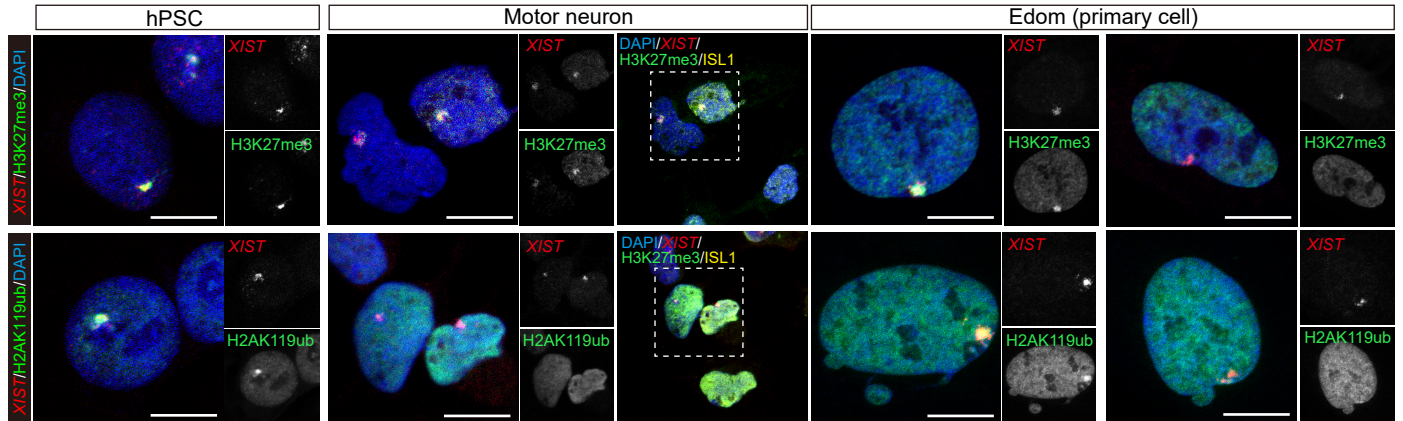
**c**



**d**



**e**



**f**

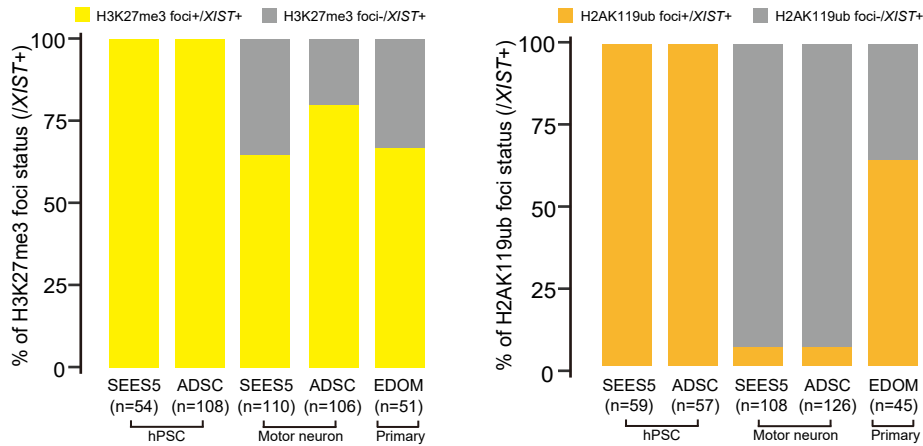




**Figure S1 related to Figure 1. Expression status of core pluripotency factors in *XIST*<sup>+</sup> and – female hPSCs and changes in epigenetic modifications on Xi in each cell type.** (a) Average X-linked gene expression status in male and female hPSCs. In females, the individual cells were separated into two groups based on the *XIST* expression status (*XIST*<sup>+</sup> or –). *p*-values were calculated using one way ANOVA with post-hoc test. (b) Expression status of core pluripotency factors. The expression statuses of OCT4, SOX2, NANOG based on *XIST* expression in each line are shown. (c) UTF1 expression status. *p*-values were calculated using the Wilcoxon's rank-sum test. (d) UTF1 and *XIST* expression status in SEES2 line. The expression levels of each gene corresponded with the heatmap. (e and f) Immuno-FISH analysis for H3K27me3, H2AK119ub, and *XIST* in hPSCs, motor neurons, and menstrual blood-derived cells (primary EDOM). Motor neurons were identified by co-staining with ISL1. Representative images (e) and quantifications results (f) are shown. n refers to the number of cells analyzed.

**Figure S2**

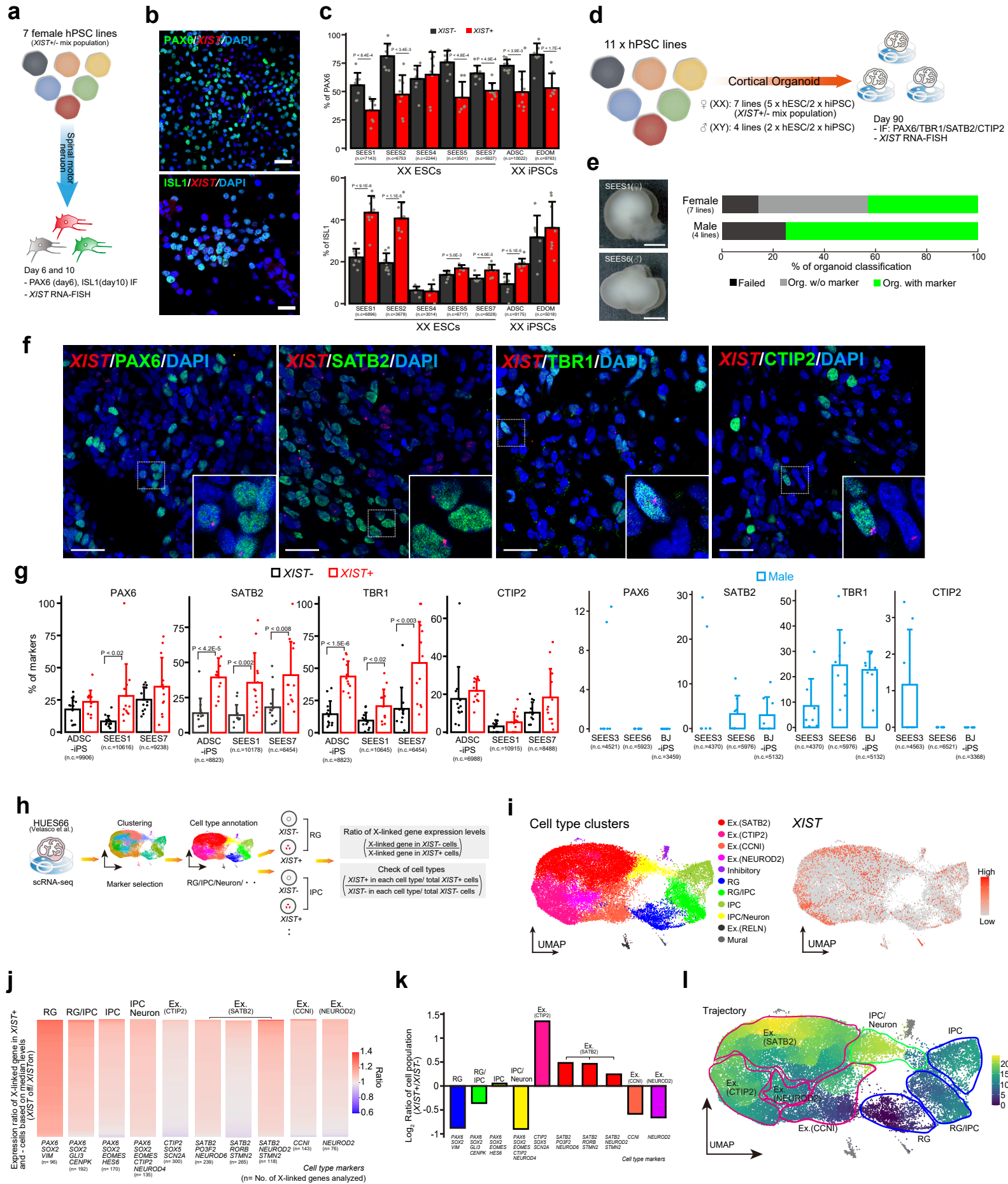


**Figure S2 related to Figure 2. *XIST* expression status is linked to the stages of neuronal differentiation.**

(a) Experimental scheme for MN differentiation from hPSCs using a 2D culture protocol. (b and c) Immunofluorescence combined with *XIST* RNA-FISH analysis in differentiating cells. The picture shows the representative image (b), and the quantification results are shown as bar graphs (c). The percentage of PAX6+ or ISL1+ cells among *XIST*+ or – cells was calculated. Each dot and n.c indicate the percentage in the observed area and the total number of cells analyzed, respectively. p-values are calculated using Student's *t*-test. Scale bar represents 50  $\mu$ m. (d) Experimental scheme for generating cortical organoids from hPSCs. On day 90, the samples were subjected to immuno-*XIST* RNA-FISH analysis. Representatives for progenitor cell (PAX6) and cortical layers (SATB2, CTIP2, and TBR1) were used. (e) Representative image of a cortical organoid and developmental summary at day 90. Scale bar represents 1 mm. (f) Representative images of immuno-*XIST* RNA-FISH analysis in cortical organoid samples. Scale bar represents 50  $\mu$ m. (g) Quantification results of each marker. In female samples, the marker expression status was based on *XIST* expression. Each dot and n.c indicate the percentage in the observed area and the total number of cells analyzed, respectively. Error bars show the standard deviation. p-values are calculated by Student's *t*-test. (h) Experimental scheme for analyzing cell types based on the *XIST* expression status in the HUES66 line (Velasco *et al.*, 2019). For analysis of the ratio of X-linked gene expression levels, X-linked genes expressed in at least 20 cells in both *XIST*+ and – groups were used. The ratios were based on the median expression levels. Each cell type annotation was based on a previous report (Bhaduri *et al.*, 2020), and the marker genes used for classifications were identified using MAST. (i) UMAP based on cell types (left) and *XIST* expression (right). RG; radial glia, IPC; intermediate progenitor cell, Ex.; excitatory. Ex. Inhibitory; inhibitory neuron. (j) Expression ratio of X-linked genes in *XIST*+ and – cells based on median levels. The heatmap shows the ratio of X-linked genes (*XIST*-/*XIST*+), indicating that red is overexpressed in *XIST*- cells. n refers to the number of X-linked genes analyzed. Representative marker genes used for the classifications are shown as cell type markers. SATB2 cells were separated into three types based on the markers. (k) The ratio of cell types based on the *XIST* expression status. Log<sub>2</sub> ratio (*XIST*+/*XIST*-) was shown in each cell type. (l) Trajectory analysis of cortical organoid. Pseudotime was calculated and the cells were highlighted based on the scores.

**Figure S3**

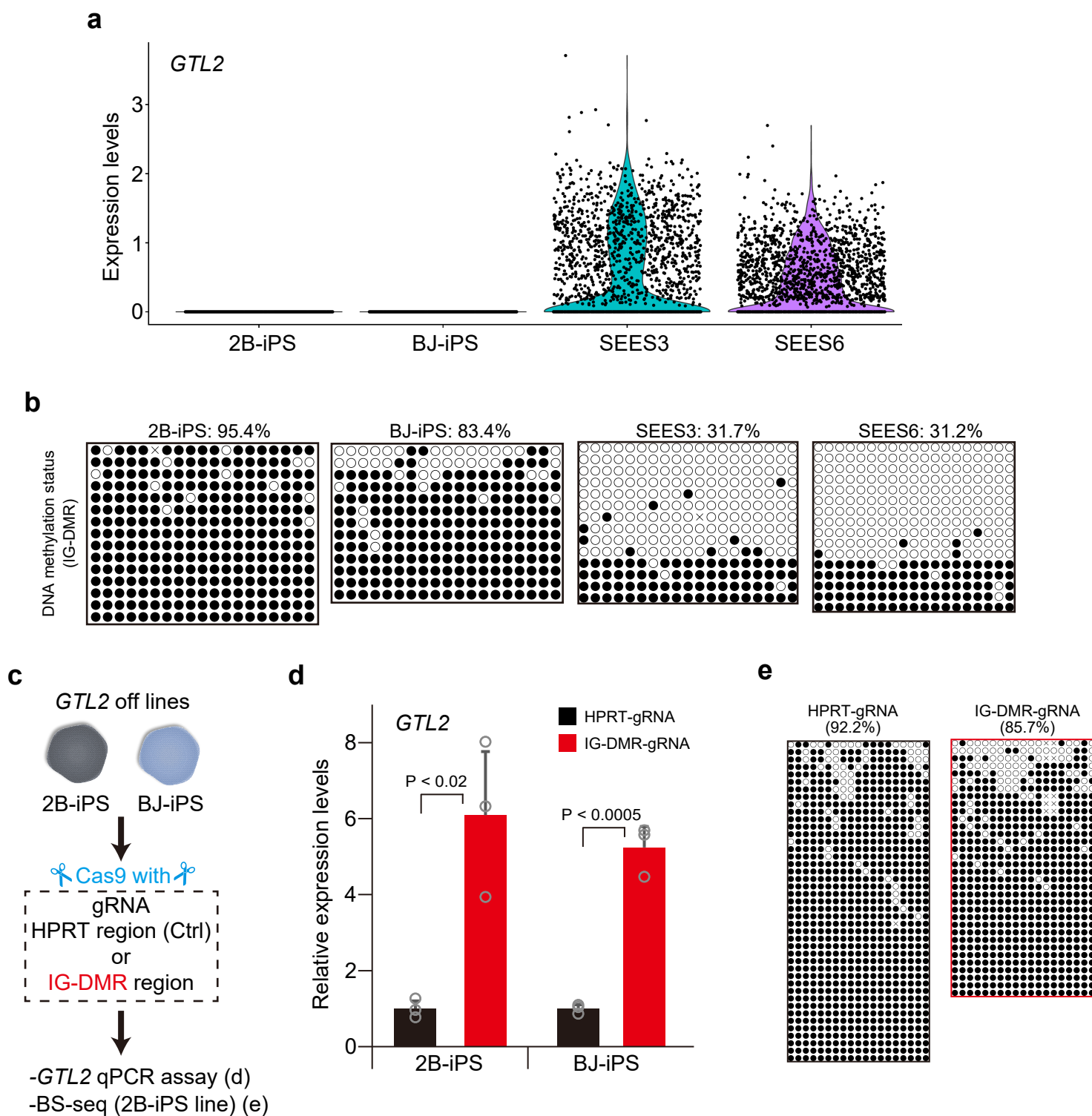
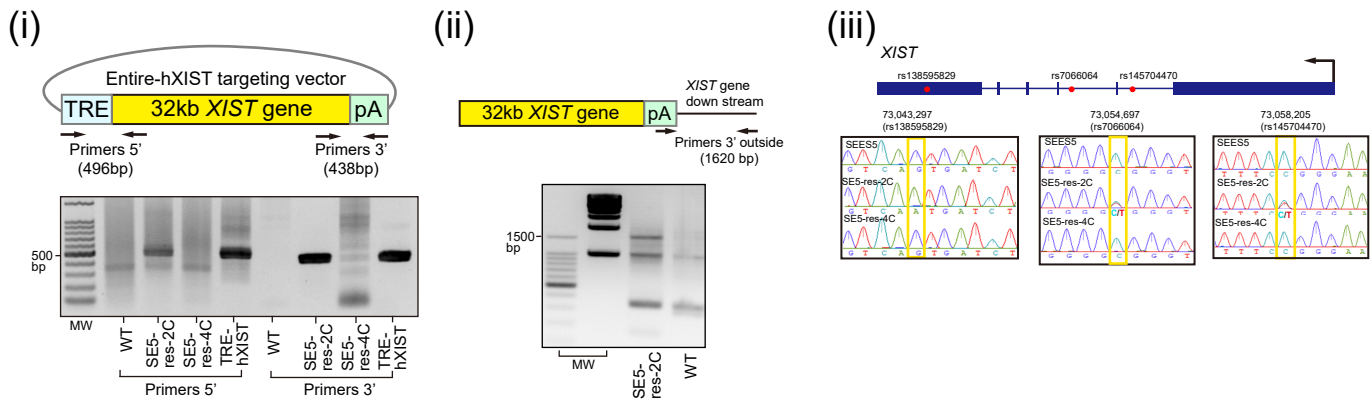


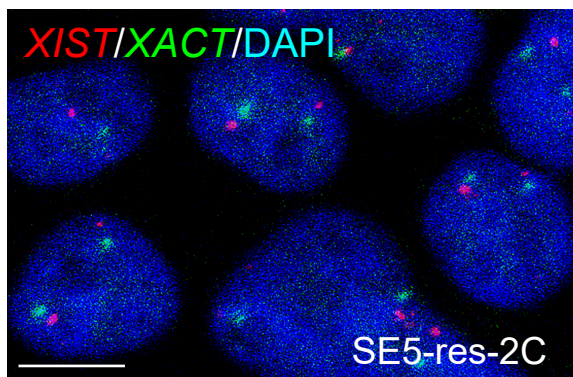
**Figure S3 related to Figure 3. Reactivation of methylated *GTL2* by Cas9-mediated DSB.** (a) *GTL2* expression in male hiPSC lines. Single-cell RNA-sequencing (scRNA-seq) data are shown. *GTL2* was not detected in hiPSC lines. (b) BS analysis of IG-DMR in *GTL2*<sup>off</sup> and *GTL2*<sup>on</sup> lines. (c) Experimental scheme for *GTL2* reactivation and DNA demethylation by Cas9-mediated DSB. *GTL2*<sup>off</sup> lines were used for the TaqMan gene expression assays (d) and BS-seq analysis (e). gRNA targeting *HPRT1* was used as a negative control. At 144 h after transfection, the cells were analyzed. (d) qPCR results for *GTL2* expression. The average expression level of the *HPRT1*-gRNA sample was set to 1 in each line. Each dot indicates an independent experiment. Error bars show the standard deviations. *p*-values were calculated using Student's *t*-test. (e) BS-seq analysis of IG-DMR in Cas9/gRNA transfected 2B-iPSCs.

# Figure S4

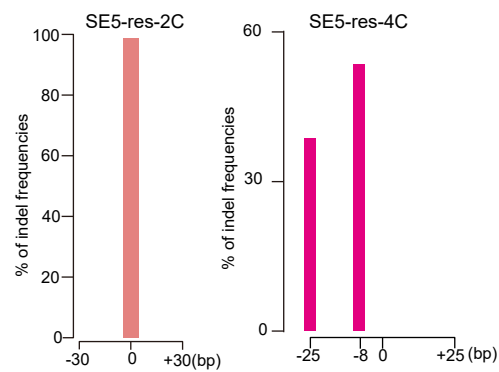
**a**



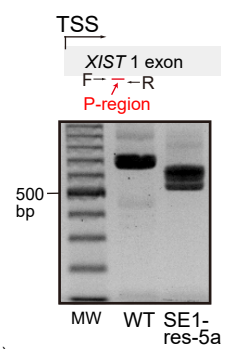
**b**



**c**



**d**

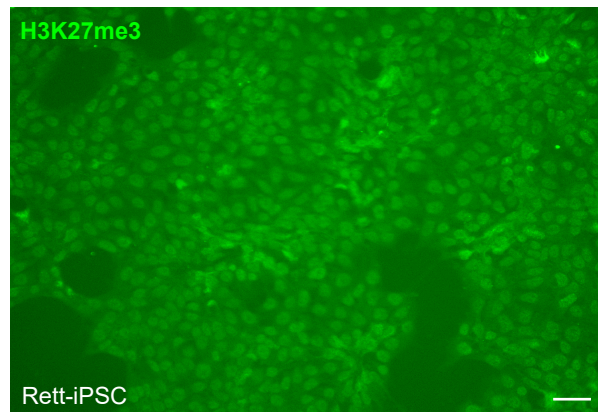


**e**

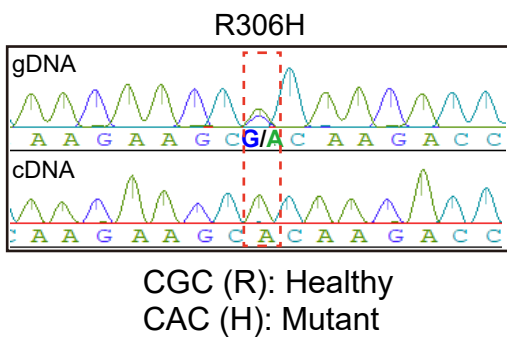
Summary of H3K27me3 rescue clones (> 85% of H3K27me3)

Lines	Recombination	P-region	
		NHEJ	Genotype
SE1-res-5a		○	Mix
SE5-res-2C	○	n.d	Homo
SE5-res-4C	n.d	○	Mix

**f**



**g**



**h**

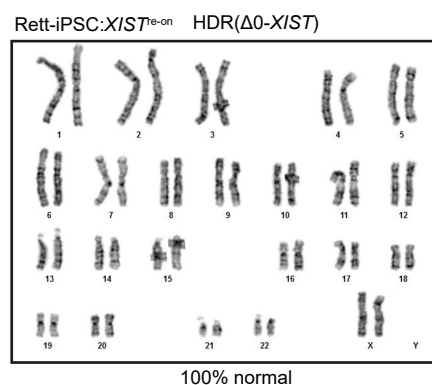




**Figure S4 related to Figure 3 and 4. Genotyping and DNAm status in *XIST* re-expressed lines and characterization of Rett-iPSCs.** (a) Genotyping PCR analysis of *XIST* re-expressing lines in SEES5 cells. TRE and SV40 sequences were included in Entire-h*XIST* vector (i and ii). Sanger sequencing analysis of SNVs (iii). (b) DNA-FISH assay using *XIST* and *XACT* probes in SE5-res-2C. The scale bar represents 10  $\mu\text{m}$ . (c) TIDE analysis for checking scars. The mutant allele was not detected in the SE5-res-2C line, whereas the SE5-res-4C line comprised cells with two different alleles. (d) Genotyping PCR spanning the P-region in SE1-res-5a. (e) Summary of the obtained H3K27me3 foci rescue clones. Mix refers to two different alleles identified by TIDE analysis or Sanger sequences. n.d. refers to not determined. (f) H3K27me3 staining of Rett-iPSC. Scale bar represents 50  $\mu\text{m}$ . (g) Genotyping and expression allele analysis using gDNA and cDNA. The mutation point is highlighted in the red dashed line. (h) G-band analysis of the Rett-iPSC: *XIST*<sup>re-on</sup> ( $\Delta 0$ -*XIST*).

# Figure 5

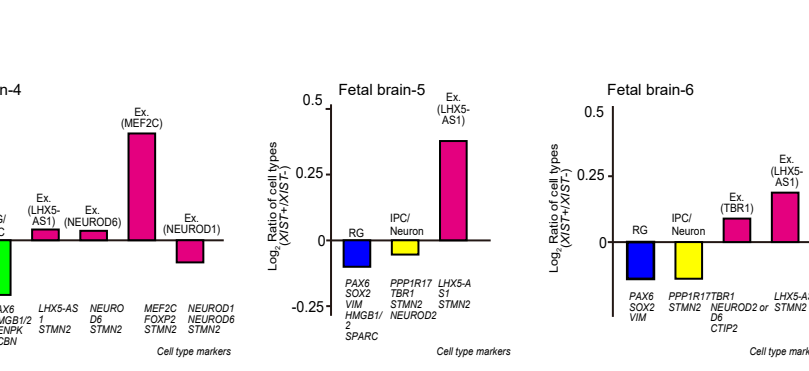
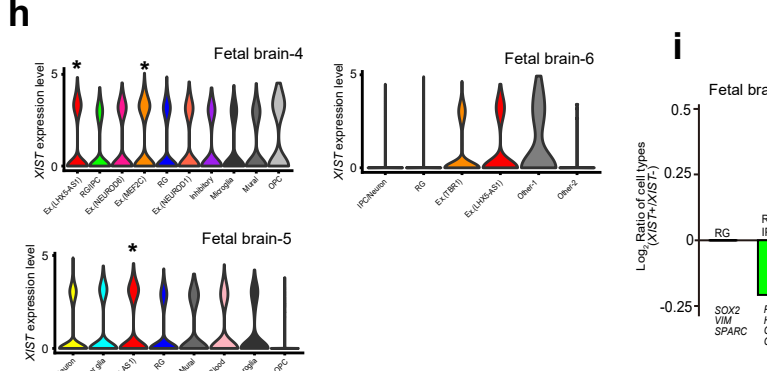
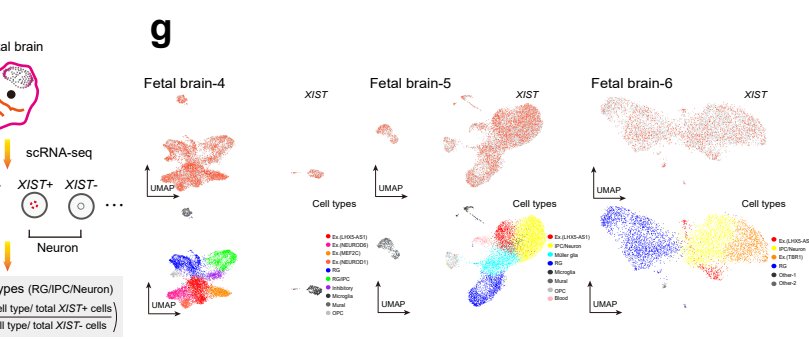
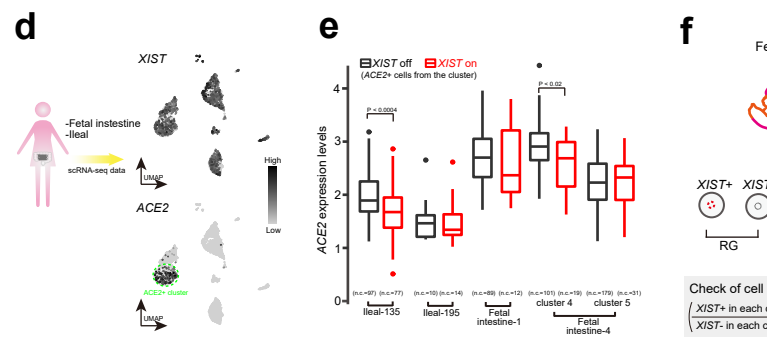
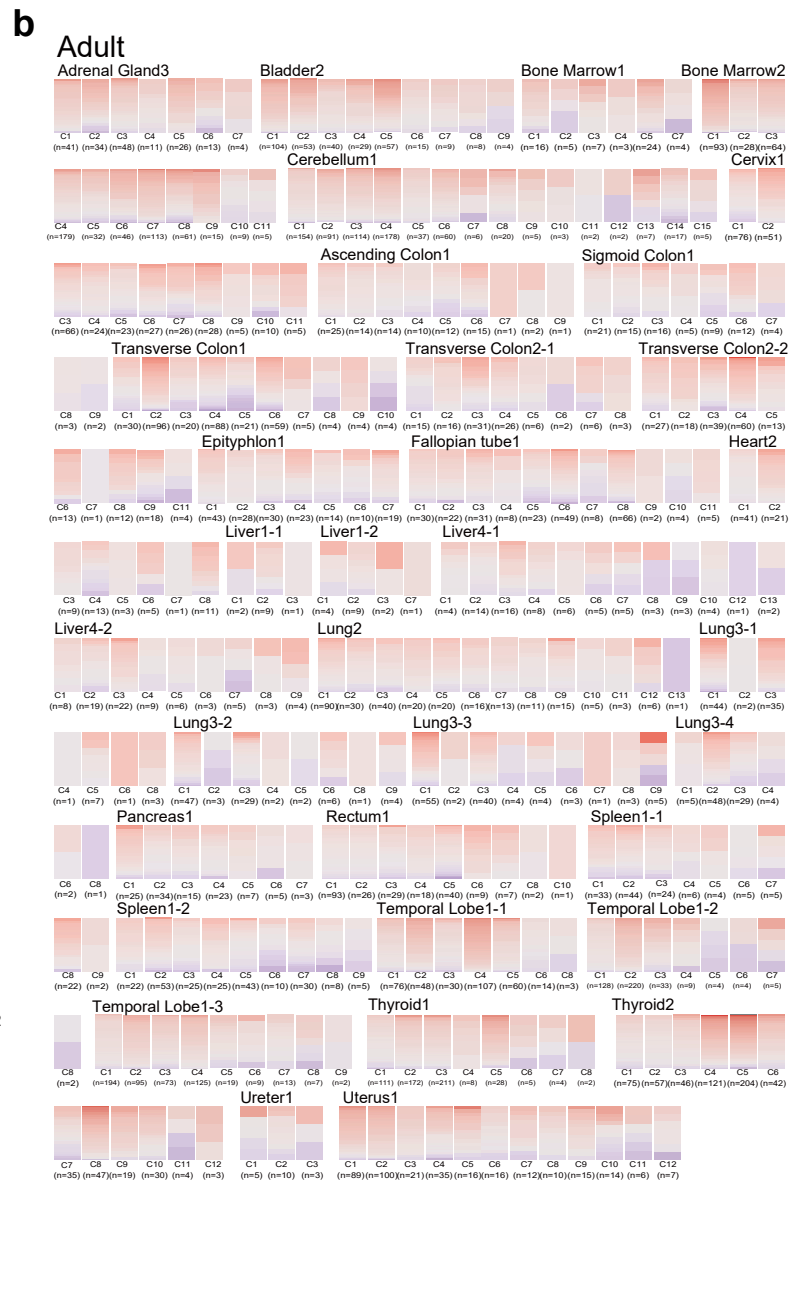
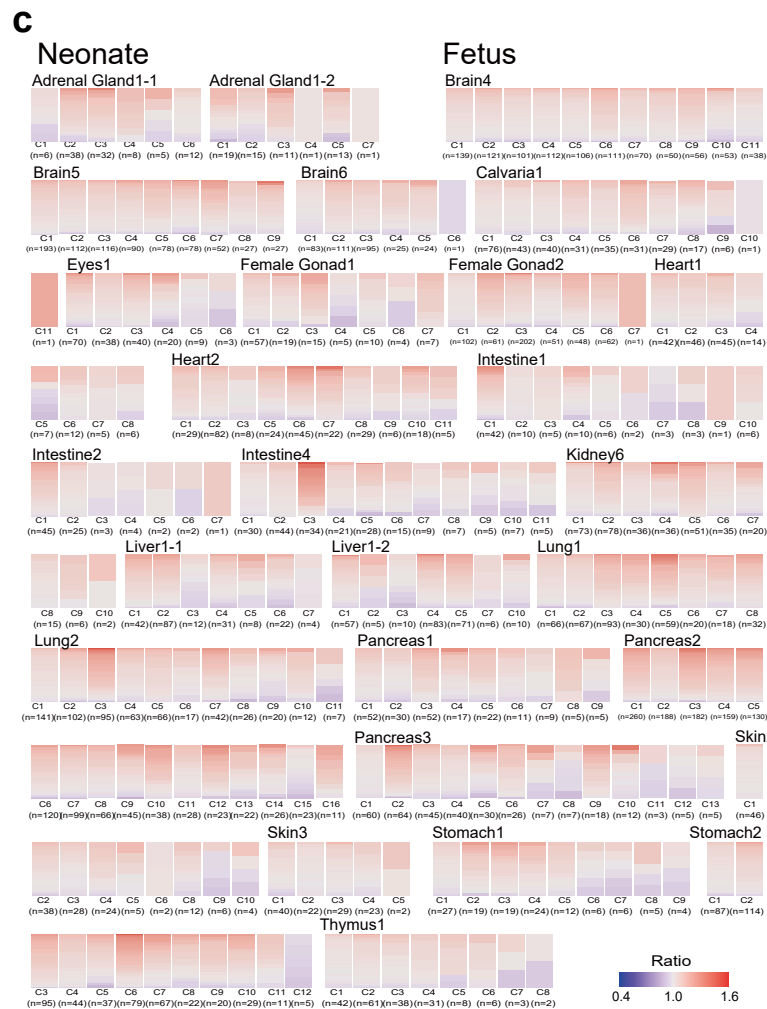
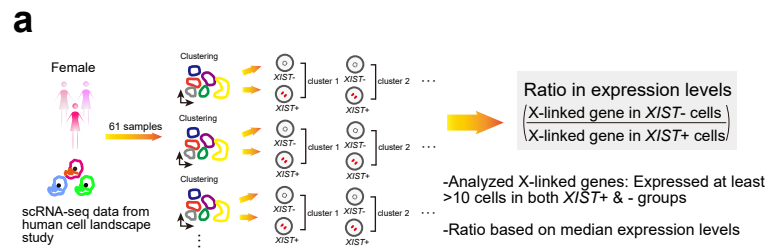


**Figure S5 related to Figure 1, 2 and 5. Effect of the *XIST* expression status *in vivo*.** (a) Analysis scheme using 61 scRNA-seq datasets from human cell atlas (Han *et al.*, 2020). (b and c) The ratios (*XIST*<sup>-</sup> cells/*XIST*<sup>+</sup> cells) in adult tissues (b) and neonatal and fetal tissues (c). C and n indicate the cluster identity and number of X-linked genes analyzed, respectively. (d) Experimental scheme for identifying *ACE2*<sup>+</sup> clusters from the fetal intestine and ileal cells. The representative images of UMAP analysis with *XIST* and *ACE2* expression are shown. The *ACE2*<sup>+</sup> clusters were identified by MAST analysis. (e) *ACE2* expression status based on the *XIST* expression levels. The cells from *ACE2*<sup>+</sup> clusters were isolated, and the *ACE2* expression levels were compared based on the *XIST* expression status. n.c. refers to the number of cells analyzed. *p*-values were calculated using the Wilcoxon's rank-sum test. (f) Experimental scheme for evaluating neuronal development *in vivo* based on the *XIST* expression status. Three fetal brain samples were used. The gene sets for cell-type annotation were identified by MAST analysis and classifications were based on the previously identified markers (Bhaduri *et al.*, 2020; Camp *et al.*, 2015). (g) UMAP analysis. The *XIST* expression status (upper) and cell types were highlighted by each color (bottom). (h) The *XIST* expression levels in each cell type based on scRNA-seq results. The violin plot shows the *XIST* expression status in each cell type. Asterisks indicate statistical significance determined using MAST test with Bonferroni correction. All *p*-values were < 7.4 E-9. (i) The ratio of cell types based on the *XIST* expression status. Log<sub>2</sub> ratio (*XIST*<sup>+</sup>/*XIST*<sup>-</sup>) was shown in each cell type. The representative marker genes used for the classification were shown.